Theoret. Comput. Fluid Dynamics (2004) 18: 97–103
Digital Object Identifier (DOI) 10.1007/s00162-004-0133-5

Theoretical and Computational Fluid Dynamics

Convective and absolute instabilities in counter-rotating spiral Poiseuille flow

J. Langenberg[1], M. Heise[1], G. Pfister[1], J. Abshagen[2]

[1] Institute of Experimental and Applied Physics, University of Kiel, 24098 Kiel, Germany
[2] Leibniz-Institute of Marine Science, University of Kiel, 24105 Kiel, Germany

Received September 26, 2003 / Accepted May 25, 2004
Published online September 7, 2004
Communicated by H.J.S. Fernando

Abstract. We present results of an experimental study on the stability of Taylor–Couette flow in case of counter-rotating cylinders and an imposed axial through flow. We are able to confirm results form recent numerical investigations done by Pinter et al. [24] by measuring the absolute and convective stability boundaries of both propagating Taylor vortices (PTV) and spiral vortices (SPI). Thus our work shows that these theoretical concepts from hydrodynamic stability in open flows apply to experimental counter-rotating Taylor–Couette systems with an imposed axial through flow.

Key words: convective and absolute instabilities, spiral Poiseuille flow
PACS: 47.20.-k, 05.45.-a, 47.15.fe

1 Introduction

The transition from the basic laminar state to turbulence in a non-equilibrium fluid flow is preferentially analyzed within the context of hydrodynamic stability theory (Swinney and Gollub [31]). Hydrodynamic instabilities and spatiotemporal pattern formation in fluid flows have been the subject of numerous experimental, numerical, and theoretical studies in the last decades (Cross and Hohenberg [9], Godreche and Manneville [13]). Hydrodynamic systems are typically classified according to their open or closed flow character. In closed flows the fluid always remain within the same physical region. By contrast, in open flows the fluid is not recycled within the physical domain of interest but leave it in a finite time. The sensitivity of many open flows to external perturbation makes it necessary to introduce the concepts of absolute and convective instabilities even for the primary instability of the basic laminar flow (Huerre and Monkewitz [16]). In the convective unstable regime the basic laminar flow becomes unstable against small perturbations but the perturbations will decay at any given stationary point in the system. Whereas in the absolute unstable case the perturbation will grow and saturate in any point so that a pattern is formed in the entire system. Examples of hydrodynamic systems where the absolute instability is superseded by a convectively unstable regime can be found in Rayleigh–Benard convection (Steinberg et al. [30]) and Taylor–Couette flow (Tagg et al. [33]).

The Taylor–Couette system consists of a viscous fluid confined in a gap between concentric rotating cylinders. The first study on hydrodynamic stability of this system has been performed by Taylor [35] Under the assumption of infinite axial length of the cylinders either stationary Taylor vortices (TVF) having an azimuthal wave number $m = 0$ or time-periodic spiral vortices (SPI) having azimuthal wave numbers $m \neq 0$

Correspondence to: G. Pfister (e-mail: pfister@physik.uni-kiel.de) occur as a result of the first pattern forming instability in basic laminar Couette flow (see e.g., Chossat [8], Swinney and Gollub [31]). Spiral vortices are travelling waves in axial and rotating waves in azimuthal direction. Krueger et al. [19] found on basis of linear stability analysis of circular Couette flow that they appear for sufficiently high counter-rotation rates. Snyder [29] was the first who observed spiral vortices in an experimental system. A systematic experimental study of counter-rotating Taylor–Couette flow has been carried out by Andereck et al. [1]. Though their investigation reveal a huge variety of different flow states that occur in the nonlinear regime away from the first instability threshold they found that only Taylor vortices and spiral vortices result from the first instability. Mode interaction between Taylor vortices and spiral vortices have been investigated numerically and experimentally by Langford et al. [20] and Tagg et al. [32] and in the context of bifurcations with symmetry by Golubitsky and Stewart [15] and Golubitsky and Langford [14]. Schulz and Pfister [28] have studied experimentally and Sanchez et al. [27] numerically the behaviour of spiral vortices in the nonlinear regime. In the 'classical' experimental configuration the Taylor–Couette system is a closed flow due to the flow domain being confined in axial direction by end plates (see e.g., in Benjamin [4] and Benjamin and Mullin [5] for the case of stationary outer cylinder). For counter-rotating cylinders Knobloch and Pierce [18] found that theoretically spiral vortices are superseded by standing wave solutions in presence of boundaries. Recently, for the first time such a behaviour has been observed experimentally by Langenberg et al. [21] but only in a small aspect ratio system. For such systems Czarny et al. [10] revealed also more complicated flow state in a numerical study.

As a result of an imposed axial through flow the character of the Taylor–Couette system changes from a closed to an open flow. The basic flow of such a system under the assumption of infinite axial length is a superposition of circular Couette and annular Poiseuille flow called Couette–Poiseuille flow (CPF). Müller et al. [23] and Recktenwald et al. [25] calculated the convective and absolute stability regimes of CPF in case of the outer cylinder being held at rest. They found that propagating Taylor vortices (PTV) result from an instability of CPF. These axisymmetric PTV propagate in the direction of the axial through flow. The effect of different boundary conditions has been investigated numerically using the Navier–Stokes equations (Büchel et al. [6]) and the Ginzburg–Landau amplitude equation (Büchel et al. [6] and Chomaz and Couairon [7]) for the transition to PTV. In agreement with more general investigations (Saarloos and Hohenberg [26] and Tobias et al. [36]) they found that size effects can be responsible for pattern selection and complex bifurcation behaviour in the absolute unstable regime. The stability boundaries of PTV have been determined experimentally by Tsamaret and Steinberg [37], Tsamaret and Steinberg [38], Babcock et al. [3], Babcock et al. [2] and Lueptow et al. [22]. In the convective unstable regime Tsamaret and Steinberg [37], Babcock et al. [3], and Babcock et al. [2] observed noise-sustained PTV with time-dependent oscillation amplitude and noisy phase. Takeuchi and Jankowski [17] studied the effect counter-rotating cylinders on the stability of CPF and found that for sufficiently high counter-rotation rate PTV are replaced by spiral vortices (SPI). Recently, Pinter et al. [24] revealed numerically that the stability boundary of CPF in counter-rotating Taylor–Couette flow also split into a convective and an absolute stability boundary for both PTV and SPI in the presence of an axial through flow.

The aim of this work is to study whether this important concept of hydrodynamic stability theory applies to experimental systems with counter-rotating cylinders and axial through flow.

2 Experimental setup

The experimental Taylor–Couette setup consists of a viscous fluid confined in the gap between two independently rotating concentric cylinders where an axial through flow is imposed. In Fig. 1a a schematic plot of the experimental apparatus is shown. The inner cylinder is machined from stainless steel having a radius of $r_\mathrm{i} = (12.50 \pm 0.01)$ mm, while the outer cylinder is made from optically polished glass with a radius of $r_\mathrm{o} = (25.00 \pm 0.01)$ mm. As a working fluid silicon oil with the kinematic viscosity $\nu = 10.04$ cSt is used. The temperature of the fluid is thermostatically controlled to (24.00 ± 0.01) °C. At top and bottom the fluid is confined by systematically riddled metal end plates which are held fixed in the laboratory frame. Their distance defines the axial height L of the flow. Both endplates have identical shape in order to assure reflection symmetry of the experimental setup. They are designed in a way that the radial and azimuthal velocity components of the axial through flow are minimized. An axial through flow is generated by a actively controlled pressure gradient between the in- and outflow at the end plates. The Reynolds number of the axial through

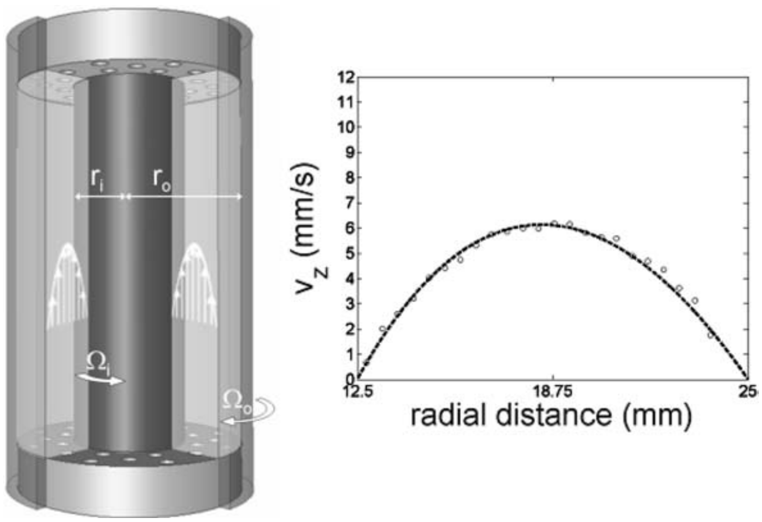

Fig. 1. (**a**) Schematic plot of the experimental apparatus. r_i and r_o denote the radius and Ω_i and Ω_o the rotation rate of inner and outer cylinder, respectively. The in- and outflow of mass in the flow domain is achieved by a pressure gradient and holes in both end plates. (**b**) analytic solution (dashed line) (Wieghardt [39]) and experimental measurements (∘) of the axial Poiseuille flow for $Re_D = 5$

flow is defined by $Re_D = d\langle v\rangle/\nu$, where $\langle v\rangle$ denote the mean axial velocity and $d = r_\mathrm{o} - r_\mathrm{i}$ the gap width. Re_D is positive for upwards and negative for downwards streaming axial through flow. As further control parameters serve the Reynolds number of the inner (i) and outer (o) cylinder, $Re_{\mathrm{i,o}} = dr_{\mathrm{i,o}}\Omega_{\mathrm{i,o}}/\nu$, where $\Omega_{\mathrm{i,o}}$ denote the rotating rate of the inner and the outer cylinder, respectively. Geometric parameters of the flow are the aspect ratio $\Gamma = L/d$ and the radius ratio $\eta = r_\mathrm{i}/r_\mathrm{o}$, which are held fixed to $\Gamma = 24.8$ and $\eta = 0.5$ for all measurements reported here. We utilize laser Doppler velocimetry (LDV) for measurements of the flow velocity and flow visualisation in order to determine spatial patterns of the flow. For all measurements the axial velocity component is recorded in the axial midplane of the system at a radial distance of 1.5 mm from the inner cylinder. The axial Poiseuille flow is well developed for all measurements presented in the present work. In Fig. 1b the analytical solution (dashed line) (Wieghardt [39]) and experimental measurements (∘) of the axial Poiseuille flow are depicted for $Re_D = 5$. Good agreement between the analytical solution and experimental results could be found.

3 Results

Flow visualisation is used in order to distinguish experimentally between propagating Taylor vortices (PTV) and spiral vortices (SPI). In Fig. 2 photographs of (a) PTV measured at $Re_D = 1.2$, $Re_\mathrm{i} = 115.7$ and $Re_\mathrm{o} = -50$ and (b) SPI measured at $Re_D = 1.0$, $Re_\mathrm{i} = 127.5$, and $Re_\mathrm{o} = -100$ are shown. Each photograph is taken in a section of the gap between the cylinders that is located in radial and axial direction symmetrically about the axial midplane. They illustrate qualitatively the field of radial and axial velocity. Note, that both photographs have been rotated in a way that the inner cylinder is located at the bottom and the outer cylinder at the top.

Figure 2a represents one vortex pair of PTV. It can be seen that in case of an axial through flow the vortex pair is no longer symmetric with respect to the outflow boundary as it is the case for a vortex pair of steady Taylor vortex flow in a ‘closed’ system. The vortex propagating ahead is larger than the other one and the core of this vortex has a larger radial distance from the inner cylinder. However, the clearly visible vortex pair characterises the appearance of PTV. In Fig. 2b the characteristic pattern of spiral vortex flow is shown. In case of spiral vortices the vortex propagating ahead is much smaller compared to the other one. No qualitative difference can be found compared to spiral vortex flow in a system without axial through flow (Schulz and Pfister [28]).

A flow in the convective and absolute unstable regime shows different dynamical behaviour. In Fig. 3 characteristic time series obtained from LDV measurements in the convective and the absolute unstable regime of PTV and SPI are shown. The measurements were performed for (a,b) $Re_\mathrm{o} = -50$ and $Re_D = 5$ and for (c,d) $Re_\mathrm{o} = -100$ and $Re_D = 1.5$. It is observed that for different Reynolds numbers of the inner cylinder two distinct dynamical regimes appear for both PTV and SPI. Below a threshold the basic state is

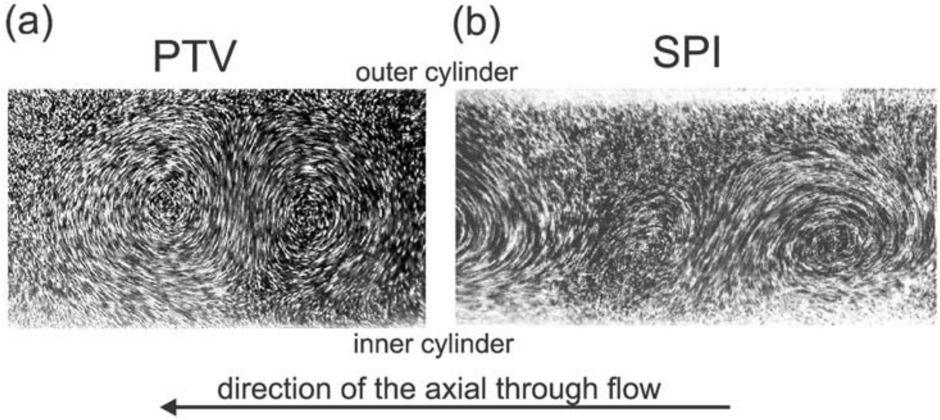

Fig. 2a,b. Photographs recorded in the (r, z)-section of the flow in the axial midplane: (**a**) Propagating Taylor vortices (PTV) for $Re_D = 1.2$, $Re_\mathrm{i} = 115.9$ and $Re_\mathrm{o} = -50$, (**b**) upwards propagating spiral vortices (SPI) for $Re_D = 1.0$, $Re_\mathrm{i} = 127.5$ and $Re_\mathrm{o} = -100$

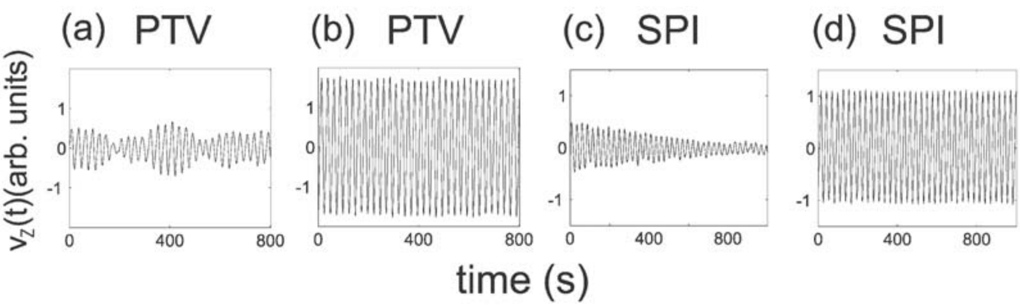

Fig. 3a–d. Time series obtained from absolute and convective unstable PTV and SPI: (**a**) convective ($Re_\mathrm{i} = 88.45$) and (**b**) absolute ($Re_\mathrm{i} = 116.7$) propagating Taylor vortices ($Re_D = 5, Re_\mathrm{o} = -50$); (**c**) convective ($Re_\mathrm{i} = 106.9$) and (**d**) absolute ($Re_\mathrm{i} = 115.7$) Spiral Vortices ($Re_D = 1.5, Re_\mathrm{o} = -100$)

absolute stable and thus neither PTV nor SPI are observed. Increasing Re_i above threshold noise-sustained structures appear. Depending on the Reynolds number of the outer cylinder these structures show characteristic properties of either PTV or SPI in flow visualisation. A typical time series of a noise-sustained PTV measured at $Re_\mathrm{i} = 88.45$ is plotted in Fig. 3a. An irregular modulation of the oscillation amplitude can be seen in the time series. Moreover, a broadening of the fundamental peak in the power spectrum is found. These are characteristic properties of a flow in a convective unstable regime. An increase of Re_i above a second threshold changes the dynamics of the PTV qualitatively. The time series recorded at $Re_\mathrm{i} = 116.7$ is plotted in Fig. 3b. The modulation of the oscillation amplitude has almost vanished and a sharp peak is found in the power spectrum of this time series. These are characteristic properties of PTV in the absolute unstable regime. Each of the two different dynamical regimes found for PTV share qualitatively dynamical properties with the corresponding SPI regime. A time series from SPI recorded in the convective unstable regime at $Re_\mathrm{i} = 106.9$ is depicted in Fig. 3c. In Fig. 3d a time series from SPI in the absolute unstable regime is plotted. The measurements were performed for $Re_\mathrm{i} = 115.7$.

Characteristic measures of the dynamics in order to characterise the transition from the absolute stable to the absolute unstable regime of PTV with increasing Re_i and to determine the convective and absolute stability threshold are depicted in Fig. 4. The measurements are performed at $Re_D = 5$ and $Re_\mathrm{o} = -50$. The mean amplitude is estimated in the experiment by the temporal mean of the maxima of the oscillations that occur in a finite velocity time series. Note, that the minima would also be suitable due to the shape of the velocity profile of PTV. The estimated mean amplitude of PTV with respect to Re_i is plotted in Fig. 4a. In the absolute stable regime the amplitude is zero and in the absolute unstable regime the amplitude has a finite value. In the convective unstable regime the amplitude varies with Re_i between almost zero and constant finite values. Note, that the measurement shown in Fig. 4a represent only one estimate of mean amplitude. Though it is an

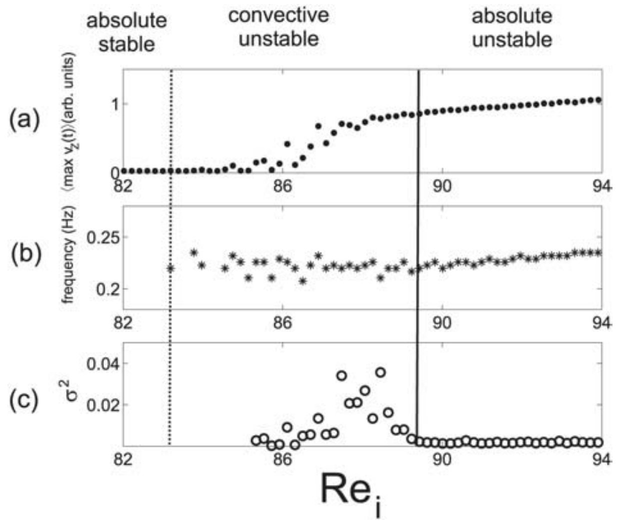

Fig. 4a–c. Characteristic properties of flow in absolute stable, convective unstable, and absolute unstable regime at $Re_D = 5$ and $Re_\mathrm{o} = -50$: (**a**) oscillation amplitude obtained from maximum of axial velocity, (**b**) oscillation frequency obtained from maximum of the fundamental peak, (**c**) variance of the fundamental peak; Experimental convective stability boundary (dashed line) is defined as appearance of fundamental peak in power spectrum while experimental absolute stability boundary (solid line) is defined as vanishing of variance of the fundamental peak

important quantity to characterise the flow it is evident for Fig. 4a that the mean amplitude does not provide an appropriate measure to determine the stability thresholds.

A better measure results from the statistical behaviour of the phase which can be determined from power spectra. The convective stability threshold is estimated in the experiment as that Re_i where the fundamental peak of the oscillation frequency can be significantly identified in the power spectrum of a time series. Note, that due to the finite length of the experimental apparatus and finite measurement time this estimate always lies above the theoretical convective stability threshold, which acts as a lower bound. The maxima of the fundamental peak are depicted in Fig. 4b as a function of Re_i. The dashed vertical line illustrates the estimate of the convective stability threshold from the measurements. Due to noise-sustained structures in the convective unstable regime the fundamental peak in the power spectrum is broadend. The absolute stability threshold is reached if the phase noise due to noise-sustained structures vanishes. The normalized variance $\sigma^2 = \langle (f - \langle f \rangle)^2 \rangle / \langle f \rangle^2$ (Babcock et al. [3]) of the fundamental peak in the power spectrum provides a measure in order to characterise such a specific behaviour. The normalized variance of the fundamental peak is depicted in Fig. 4c. We have illustrated the estimated value of Re_i for the absolute stability threshold by a solid vertical line. Note, that close to the absolute stability threshold in the convective unstable regime the modulation of the oscillation amplitude is already very small though the phase is still noisy. In Fig. 5 we present experimental measurements for the convective and absolute stability boundaries of (a) propagating Taylor vortices (PTV) for $Re_\mathrm{o} = -50$ and of (b) spiral vortices (SPI) for $Re_\mathrm{o} = -100$ in a Taylor–Couette flow with an imposed axial through flow. Moreover, the numerically results calculated by Pinter et al. [24] are plotted in Fig. 5. The dashed lines represent the convective and the solid lines the absolute stability boundary. It can be seen that the convective unstable regime becomes larger with increasing Re_D. The experimental measurements of the convective stability boundary of PTV and SPI are always close but systematically above the numerical values. This is intrinsic to the experimental method due to the finite extension of the apparatus

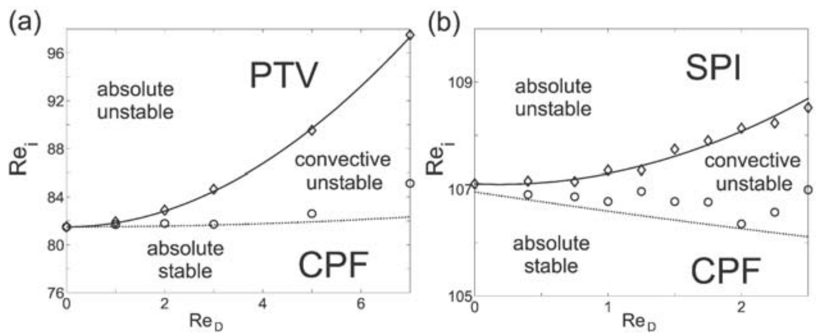

Fig. 5a,b. (**a**) Numerical convective (dashed line), experimental convective (○), numerical absolute (solid line) and experimental absolute (◇) stability thresholds of (**a**) PTV ($Re_\mathrm{o} = -50$) and (**b**) SPI ($Re_\mathrm{o} = -100$)

and the finite measurement time. However, a reasonable quantitative agreement between numerical results and experiments can be found for both PTV and SPI for small Re_D. The experimental measurements of the absolute stability boundary are found to be in quantitative agreement with the numerical results for the transition to PTV and SPI from Pinter et al. [24] for all Re_D.

4 Conclusion

We have examined experimentally the effect of an imposed axial through flow on the transition to axisymmetric propagating Taylor vortices and non-axisymmetric spiral vortices in a counter-rotating Taylor–Couette flow. This work is motivated by recent numerical calculations done by Pinter et al. [24] who determined the convective and absolute stability thresholds of basic Couette–Poisseuille flow under the assumption of infinite axial height. We are able to confirm the numerical results for an experimental system with open flow boundaries by measuring the absolute and convective stability threshold of both propagating Taylor vortices (PTV) and spiral vortices (SPI). The convective and the absolute stability thresholds has been determined due to the height and the normalized variance of the fundamental peak in the power spectrum, respectively. The agreement is quantitative in case of absolute stability and reasonable quantitative but systematically biased in case of convective stability due to experimental limitations related to the noise-sustained behaviour of PTV or SPI.

Our work shows that the theoretical concepts of convective and absolute hydrodynamic stability in open flows apply to experimental counter-rotating Taylor–Couette systems with an imposed axial flow through open boundaries.

Acknowledgments. We thank Wolfgang Schumann and Heinz Horak for the technical support. The authors gratefully acknowledge support from the 'Deutsche Forschungsgemeinschaft' (JL and GP: research grant No. PF 210/10-1; JA: SFB460).

References

1. Andereck, C.D., Lui, S.S., Swinney, H.L.: Flow regimes in a circular Couette system with independently rotating cylinders. J. Fluid Mech. **164**, 155–183 (1986)
2. Babcock, K.L., Ahlers, G., Cannell, D.S.: Noise-sustained structure in Taylor–Couette flow with through flow. Phys. Rev. Lett. **67**, 3388–3391 (1991)
3. Babcock, K.L., Ahlers, G., Cannell, D.S.: Noise amplification in open Taylor–Couette flow. Phys. Rev. E **50**, 3670–3692 (1994)
4. Benjamin, T.B.: Bifurcation phenomena in steady flows of liquid. I. Theory. Proc. R. Soc. A (London) **359**, 1–26 (1978)
5. Benjamin, T.B., Mullin, T.: Anomalous modes in Taylor–Couette flow. Proc. R. Soc. A (London) **377**, 221–249 (1981)
6. Büchel, P., Lücke, M., Roth, D., Schmitz, R.: Pattern selection in the absolutely unstable regime as nonlinear eigenvalue problem: Taylor vortices in axial flow. Phys. Rev. E **53**, 4764–4777 (1996)
7. Chomaz, J.M., Couairon, A.: Against the wind. Phys. Fluids **11**, 2977–2983 (1999)
8. Chossat, P., Iooss, G.: *The Couette–Taylor Problem*. Springer-Verlag (1994)
9. Cross, M.C., Hohenberg, P.C.: Pattern formation outside from equilibrium. Rev. Mod. Phys. **65**, 851 (1993)
10. Czarny, O., Serre, E., Bontoux, P., Lueptow, R.M.: Spiral and wavy vortex flows in short counter-rotating Taylor–Couette cells. Theoret. Comput. Fluid Dynamics **16**, 5–15 (2002)
11. Edwards, W.S., Tagg, R., Dornblaser, B.C., Swinney, H.L., Tuckerman, L.S.: Periodic traveling waves with nonperiodic pressure. Phys. Eur. J. Mech. B/Fluids **10**, 205–210 (1991)
12. Egbers, C., Pfister, G. (eds.): *Physics of rotating fluids*. Springer-Verlag (2000)
13. Godreche, C., Manneville, P.: *Hydrodynamics and nonlinear instabilities*. Camebridge University Press (1998)
14. Golubitsky, M., Langford, W.F.: Pattern formation and bistability in flow between counterrotating cylinders. Physica D **32**, 362–392 (1988)
15. Golubitsky, M., Stewart, I.: *The Symmetry Perspective*. Birkhäuser-Verlag (2002)
16. Huerre, P., Monkewitz, P.A.: Hopf bifurcation with broken circular symmetry. Ann. Rev. Fluid. Mech. **22**, 357–473 (1990)
17. Takeuchi, D.I., Jankowski, D.F.: A numerical and experimental investigation of the stability of spiral Poiseuille flow. J. Fluid. Mech. **102**, 101–126 (1980)
18. Knobloch, E., Pierce, R.: Spiral vortices in finite cylinders. In: Andereck, C.D., Hayot, F. (eds.) *Ordered and turbulent patterns in Taylor–Couette flow*. Nato ASI Series (1992)
19. Krueger, E.R., Gross, A., Di Prima, R.C.: On the relative importance of Taylor-vortex and non-axisymmetric modes in flow between rotating cylinders. J. Fluid Mech. **24**, 521–538 (1966)

20. Langford, W.F., Tagg, R., Koestlich, E.J., Swinney, H.L., Golubitsky, M.: Primary instabilities and bicriticality in flow between counter-rotating cylinders. Phys. Fluids **31**, 776–785 (1987)
21. Langenberg, J., Pfister, G., Abshagen, J.: Standing waves in flow between counter-rotating cylinders. To be published in Phys. Rev. E (2003)
22. Lueptow, R.M., Doctor, A., Kyungyoon, M.: Stability of axial flow in an annulus with a rotating inner cylinder. Phys. Fluids A **4**, 2446–2455 (1992)
23. Müller, H.W., Lücke, M., Kamps, M.: Convective patterns in horizontal flow. Eur. Phys. Lett. **10**, 451 (1989)
24. Pinter, A., Lücke, M., Hoffmann, C.: Spirals and Taylor vortex fronts and pulses in axial through-flow. Phys. Rev. E **67**, 26318–26333 (2003)
25. Recktenwald, A., Lücke, M., Müller, H.W.: Taylor vortex formation in axial through-flow: Linear and weakly nonlinear analysis. Phys. Rev. E **48**, 4444–4454 (1993)
26. Saarloos, W., van Hohenberg, P.C.: Fronts, pulses, sources and sinks in generalized complex Ginzburg–Landau equation. Physica D **56**, 303–367 (1992)
27. Sanchez, J., Crespo, D., Marques, F.: Spiral vortices between concentric cylinders. Appl. Sci. Res. **51**, 55–59 (1993)
28. Schulz, A., Pfister, G.: In: Egbers, C., Pfister, G. (eds.) *Physics of rotating fluids*. Springer-Verlag (2000)
29. Snyder, H.A.: Stability of Rotating Couette Flow. I. Asymmetric waveforms. Phys. Fluids **11**, 728–734 (1968)
30. Steinberg, V., Fineberg, J., Moses, E., Rehberg, I.: Pattern selection and transition to turbulence in propagating waves. Physica D **37**, 359–383 (1989)
31. Swinney, H.L., Gollub, J.P.: *Hydrodynamic instbilities and the transition to turbulence*. Springer-Verlag (1981)
32. Tagg, R., Edwards, W.S., Swinney, H.L., Marcus, P.S.: Nonlinear standing waves in Couette–Taylor flow. Phys. Rev. A **39**, 3734–3737 (1989)
33. Tagg, R., Edwards, W.S., Swinney, H.L.: Convective versus absolute instability in flow between counterrotating cylinders. Phys. Rev. A **42**, 831–837 (1990)
34. Tagg, R.: *The Taylor–Couette Problem*. Non. Sci. Today **4** (1994)
35. Taylor, G.I.: Stability of a viscous liquid contained between two rotating cylinders. Philos. Trans. R. Soc. London, Ser. A, **223**, 289–343 (1923)
36. Tobias, S.M., Proctor, M.R.E., Knobloch, E.: Convective and absolute instabilities of fluid flows in finite geometry. Physica D **113**, 43–72 (1998)
37. Tsamaret, A., Steinberg, V.: Noise modulated-propagating pattern in a convectively unstable system. Phys. Rev. Lett. **67**, 3392–3395 (1991)
38. Tsamaret, A., Steinberg, V.: Competing states in a Couette–Taylor system with an axial flow. Phys. Rev. E **49** 4077–4086 (1993)
39. Wieghardt, K.: *Theoretische Strömungslehre*. Teubner-Verlag (1974)